REPORT DOCUMENTATION PAGE

1. AGENCY USE ONLY (Leave Blank)	2. REPORT DATE Jan. 16, 2001	3. REPORT TYPE AND DATES COVERED Final Progress, 06/01/97 to 05/31/00

4. TITLE AND SUBTITLE
High Temperature AL-Nanocrystal Alloy Synthesis

5. FUNDING NUMBERS
DAAG55-97-1-0149

6. AUTHOR(S)
Professor J.H. Perepezko

7. PERFORMING ORGANIZATION NAME(S) AND ADDRESS(ES)
University of Wisconsin-Madison
Department of Materials Science and Engineering
1509 University Ave.
Madison, WI 53706

8. PERFORMING ORGANIZATION REPORT NUMBER

9. SPONSORING / MONITORING AGENCY NAME(S) AND ADDRESS(ES)

U. S. Army Research Office
P.O. Box 12211
Research Triangle Park, NC 27709-2211

10. SPONSORING / MONITORING AGENCY REPORT NUMBER

ARO 37157.1-MS-AAS

11. SUPPLEMENTARY NOTES

12 a. DISTRIBUTION / AVAILABILITY STATEMENT

Approved for public release; distribution unlimited.

12 b. DISTRIBUTION CODE

13. ABSTRACT (Maximum 200 words)

Aluminum-rich metallic glasses containing transition metals and rare earth elements have been found to yield finely mixed microstructures of Al nanocrystals embedded in an amorphous matrix and exhibit enhanced fracture strength with several percent strain. Upon primary crystallization of melt spun ribbons, this novel microstructure comprised of a high particle density ($> 10^{20}$ m^{-3}) of Al nanocrystals (20nm) in an amorphous matrix develops and offers exceptional strength (1500MPa) and high temperature stability (533K). Numerical modeling based upon the size distribution of the Al nanocrystals after isothermal annealing is applied to study the nucleation kinetics in the metallic glasses. In addition to the kinetic study of primary nanocrystallization, the glass transition temperature (T_g) has been assessed in Al-7at%Y-5at%Fe and Al-8at%Sm alloys. In usual calorimetric measurements, the thermal response of the primary crystallization often obscures the observation of the signal corresponding to the glass transition. As a result, T_g is often assumed to be near the onset of the primary crystallization reaction (T_x^{Al}). However, it has been demonstrated by modulated-temperature calorimetry that this assumption does not apply strictly to the metallic glasses under study. The thermal stabilization of the microstructure by the occurrence of diffusion field impingement allows for the observation of the glass transition of the remaining amorphous phase in the matrix by modulated DSC. The reliable assessment of the glass transition temperature provides not only a fundamental basis for the kinetics analysis, but also an important parameter in designing suitable annealing treatments that allow for the development of desired microstructures to yield optimized properties.

14. SUBJECT TERMS
Aluminum alloys, nanocrystalline, metallic glass, crystallization kinetics, nucleation, modulation calorimetry

15. NUMBER OF PAGES
8

16. PRICE CODE

17. SECURITY CLASSIFICATION OR REPORT UNCLASSIFIED	18. SECURITY CLASSIFICATION ON THIS PAGE UNCLASSIFIED	19. SECURITY CLASSIFICATION OF ABSTRACT UNCLASSIFIED	20. LIMITATION OF ABSTRACT UL

NSN 7540-01-280-5500

20010227 145

4. Scientific Progress and Accomplishments

1. Introduction

Recently, Al-based nanostructured alloys have attracted considerable attention due to their attractive potential in structural applications. These metallic glasses have demonstrated outstanding mechanical properties such as ultrahigh tensile strength with respect to their density [1-4]. Rapid solidification processing such as melt-spinning is the most commonly applied technique in producing metallic glasses [2-5]. The high cooling rate (10^5 to 10^6 Ks^{-1}) achievable by this technique enables the suppression of crystallization in some alloy systems and results in the formation of ribbons with a fully amorphous structure as judged by TEM and XRD observations [5]. The appearance of an endothermic response during heating by differential scanning calorimetry (DSC) is generally indicative of the existence of a glassy state [6,7]. However, this does not apply to some marginal glass forming systems such as Al-Y-Fe and Al-Sm where the glass transition signal is obscured by the exothermic thermal response from the primary crystallization of Al upon heating [8-11]. Thus, direct evidence for the formation of a glassy state in these alloys was not obtained by conventional calorimetry. Nevertheless, the establishment of a reliable approach to assess the glass transition temperature for this type of metallic glass is necessary in providing a fundamental basis for an analysis of the transformation kinetics [10]. Often, the onset temperature of the primary crystallization is taken as an estimate for the glass transition temperature [10,12]. However, it is difficult to verify experimentally the accuracy of this assumption since the onset temperature is often not sharp and has been reported to span a relatively wide temperature range. The application of modulated-temperature differential scanning calorimetry (DDSC) is presented in the current study to demonstrate the capability to assess the glass transition temperature by distinguishing the endothermic response due to the glass transition from the exothermic signal due to the crystallization reaction.

Though the occurrence of primary crystallization may impede the direct observation of the glass transition in some Al-base metallic glasses, it does offer an important opportunity in synthesizing nanostructured materials through the formation of microstructures with finely dispersed nanocrystalline Al in an amorphous phase. It has been reported that a homogeneous dispersion of the nanocrystalline Al particles embedded in the amorphous matrix has increased the tensile strength substantially to 1500MPa, which is higher than the strength for single-phase amorphous alloys [13-21]. The enhanced mechanical properties displayed by nanocrystalline amorphous alloys indicate an attractive potential for their commercial applications as structural materials. It has been suggested that the superior mechanical properties can be attributed to the enhancement of the resistance to shear deformation caused by the nanoscale Al particles. The nanoscale fcc-Al particles are smaller than the thickness of the shear deformation band in the amorphous alloy and can act as an effective barrier against the subsequent deformation of the amorphous matrix [21, 22]. The capability to control the nucleation density is one of the important issues in the controlled synthesis of nanocrystalline Al microstructures. The crystallization behavior in these Al-based amorphous alloys can be evaluated by numerical modeling of the kinetics based upon the measured size distribution of the Al nanocrystals in the partially devitrified samples after isothermal annealing.

2. Experimental Procedures

Alloys with nominal compositions of Al-7at%Y-5at%Fe, Al-8at%Sm were prepared by a two-step process. Bulk ingots of suitable compositions were produced by repeated arc-melting the mixture of high purity elements (Al: 99.999%; Y: 99.9%; Fe: 99.995%) on a water-cooled copper hearth in an argon-protected environment to ensure complete melting and compositional homogeneity. A titanium button was melted prior to alloy melting to react with residual oxygen and nitrogen in the chamber. Amorphous ribbons were produced by a single-roller melt-spinning facility at a tangential wheel speed of 33m/s in an argon-controlled environment. The ingots were induction-melted in a quartz crucible and then ejected onto the copper wheel by high-pressure argon. The approximate width and thickness of the melt-spun ribbons are 3mm and 40 μm, respectively. The structural characterization of the samples was performed by standard X-ray diffraction (XRD, Philips XRD) in reflection mode using Cu-K$_\alpha$ radiation. Microstructural characterization was carried out by transmission

electron microscopy / selected area electron diffraction (TEM/SAED) on a Philips CM200 with standard thinning procedures in a Gatan 600 ion miller. The amorphous samples were devitrified in a differential scanning calorimeter (DSC) by rapid heating to the annealing temperatures followed by isothermal annealing. The particle size and volume fraction of the Al nanocrystals in different partially crystallized samples were determined from TEM bright-field micrographs with image analysis software (Image-Pro). Calorimetric signals from phase transformations during heating at low rates were monitored by DSC using a Perkin-Elmer DSC-7 system at constant heating rate. Temperature-modulated calorimetry was performed by using the DSC in the dynamic (DDSC) mode. In this mode, the response of the sample to a time-dependent signal (sinusoidal temperature change) is measured. That is, a periodically varying temperature oscillation is superimposed on a constant heating or cooling rate. The response signal consists of the superposition of two independent signals: the underlying heat flow that corresponds to the conventional DSC signal [23] and an oscillating heat flow. Contributions to the calorimetric signal of a sample due to a change of the specific heat such as e.g. the glass transition are observed on the dynamic response signal. In contrast, slow transformations or reactions such as the primary crystallization, which proceed independently from the temperature modulation, contribute to the underlying static heat-flow. In the framework of the linear response theory, the response function to an oscillatory attenuation consists of two contributions that are in and out of phase with respect to the input signal. Using complex notation for the vector sum of the contributions to the dynamic specific heat signal gives:

$$C(\omega) = C'(\omega) - iC''(\omega) \qquad\qquad (1)$$

Where $C(\omega)$ is the frequency-dependent complex specific heat; $C'(\omega)$ is the real part or storage specific heat; and $C''(\omega)$ is the imaginary part or loss specific heat [24]. While dissipative processes such as the relaxation of the glassy state contribute to the imaginary part, C'' (the loss heat capacity), the molecular motions i.e. the molecular rearrangement that occurs during a glass transition contribute to the real part C' (storage heat capacity). Thus both, C' and C'' are affected by a glass transition that occurs in the sample.

3. Results and Discussion

The TEM bright-field image of an $Al_{88}Y_5Fe_7$ as-spun ribbon sample in Figure 1-a does not display any perceptible crystallites indicating a homogeneous and fully amorphous structure. The corresponding selected area electron diffraction (SAED) pattern shown in the inset exhibits a diffuse ring that also suggests that the ribbon sample is amorphous. However, the DSC trace in Figure 1-b of an $Al_{88}Y_5Fe_7$ as-spun ribbon sample during heating at 40K/min does not show the glass transition. The XRD results on the samples that were heated to temperatures before and after the first exothermic peak indicate that the reaction corresponds to the formation of a primary α-Al nanocrystalline phase from the amorphous matrix. The microstructural characterization and thermal analysis by DSC on the $Al_{92}Sm_8$ as-spun samples yielded the same results. In order to ensure the structural identity of the amorphous phase in these melt-spun ribbons, modulated-temperature DSC (DDSC) analysis has been carried out. The results of modulation calorimetry experiments on the as-spun ribbon materials are shown in Figure 2 in comparison to the DSC trace obtained from the underlying static heat flow. The exothermic signal that corresponds to the non-reversible primary crystallization process is excluded by the time series analysis of the modulated heat flow signal and the endothermic signal due to the glass transition is observed in the storage and loss specific heat curves at about 531K for $Al_{88}Y_7Fe_5$ (Figure 2-a) and 445K for $Al_{92}Sm_8$ (Figure 2-b), respectively [25]. The transition due to crystallization that occurs at 498K in Figure 2-b develops too rapidly to be excluded by the Fourier analysis. Also, the linear response theory does not apply here since the sample is far from local equilibrium. As a result, the storage heat capacity curve displays an abrupt change that is not given by the linear response theory. The difference in the onset temperature of the primary crystallization shown in Figure 2-a and Figure 1 is due to the different underlying heating rates (DDSC: 2K/min). The DDSC results confirm that a glassy state has actually been achieved during the melt-spinning process on the alloys. The calorimetric signal of the glass transition in the conventional continuous heating DSC is actually concealed by the heat release from the primary crystallization reaction.

However, it has been reported that upon heating the Al-Y-Fe as-spun ribbons with similar compositions prepared at a higher melt-spinning rate, a clear glass transition was observed and is well-separated from the

2

crystallization temperature in DSC [26]. The distinction in the thermal response of the as-spun amorphous ribbons that were prepared at different wheel speed during melt-spinning makes it necessary to identify the mechanism of the metallic glass formation. Figure 3 shows a schematic illustration to highlight the difference between the two controlling mechanisms in metallic glass formation: nucleation control vs. growth control. The key issue in forming metallic glass by rapid solidification is the suppression of crystallization during rapid quenching. Under nucleation control, the cooling path bypasses the nucleation reaction and the cluster distribution that may be retained during quenching process does not overlap with the critical nucleus size at the crystallization temperature (T_x). As a result, a clear separation in temperature between the glass transition temperature (T_g) and T_x can be observed during reheating. With growth control, some small fraction of crystallites may form initially during rapid quenching, but the viscosity that increases rapidly with decreasing temperature near T_g prevents their growth. Most importantly, under growth control the cluster distribution that is retained overlaps with the critical nucleation size at T_g. In either case, upon heating rapid crystallization occurs at T_g which will essentially coincide with T_x. As the model suggests, the observation of a clear glass transition in the as-spun ribbons fabricated at a higher wheel speed is the result of the alteration in the controlling mechanism during glass formation from growth control to nucleation control.

The TEM bright field image in Figure 4-a shows that a high number density ($3\times10^{21}m^{-3}$) of nearly spherical Al nanocrystals has developed in an $Al_{88}Y_7Fe_5$ melt-spun sample after annealing at 518K for 10 minutes. Similar results have been found in the samples that were isothermally annealed at 508K. This result indicates that Al nanocrystals develop slowly at temperatures below the calorimetrically determined crystallization onset (546K). The growth kinetics of the primary crystallization in the amorphous alloy has been analyzed considering spherical precipitate growth including diffusion-field impingement [10]. At early stages during isothermal annealing when the Al nanocrystals are very small and the diffusion fields do not overlap, the crystallites are nearly spherical (Figure 4-a). The growth is governed by diffusion control, which can be expressed by a parabolic function ($R \propto \sqrt{Dt}$, R = radius of the nanocrystal; D = matrix diffusivity; t = growth time). As further growth of nanocrystals proceeds, the interparticle spacing decreases and the development of a solute buildup around the nanocrystals eventually leads to the overlap of the diffusion fields, and consequently retards the further advancement of the growth front significantly [27, 28]. Moreover, the interface between the Al nanocrystals and the amorphous matrix becomes irregular or dendritic as perturbations develop into the amorphous matrix which is effectively a highly undercooled liquid. The development of a dendritic morphology for the Al nanocrystals after longer annealing time is shown in Figure 4-b. Furthermore, the solute enriched remaining amorphous matrix may decrease the diffusivity of the solute and can lead to a higher crystallization temperature range for the residual amorphous phase that offers higher thermal stability [29, 30].

A nucleation study was carried out on the partially devitrified $Al_{88}Y_7Fe_5$ samples. Short period isothermal annealing treatments were applied to avoid possible diffusion-field impingement that occurs at later stages [27, 30]. The analytical expression of heterogeneous transient nucleation by Kashchiev [31] was applied here:

, where $N_V(t)$ is the number of Al nanocrystals per unit volume of the sample, J_{st} is the steady state heterogeneous nucleation rate, τ is the time lag. Figure 5 shows the result of numerical calculation based on the size distribution of Al nanocrystals from an $Al_{88}Y_7Fe_5$ melt-spun sample that was isothermally annealed at

$$N_V(t) = J_{st}\left[t - \frac{\pi^2}{6}\tau - 2\tau\sum_{n=1}^{\infty}\frac{(-1)^2}{n^2}\exp\left(-n^2\frac{t}{\tau}\right)\right] \quad (2)$$

518K for 10 min. The nucleation density at different times before diffusion field impingement is determined by correcting the measured nanocrystal density for diffusional growth [32, 33]. The estimated steady state heterogeneous nucleation rate (J_{st}) following a transient period is about 5×10^{19} $m^{-3}s^{-1}$. It appears that the heterogeneous transient nucleation is more likely to be the mechanism for nucleation during the primary crystallization of the metallic glass. This agrees with the high density of heterogeneous nucleation sites observed in droplet experiments of the alloy [34]. Recently, a comparison study on the Al-Sm amorphous alloy prepared independently by rapid solidification process (i.e. melt-spinning) and solid state amorphization (i.e.

cold rolling) suggests that the high density quenched-in nuclei actually originate from the rapid quenching process [35, 36]. It is evident that the key issue in synthesizing amorphous alloys with a high density of Al nanocrystals is the capability to control the nucleation density which appears to be closely related to the kinetics for the development of quenched-in clusters which will be treated in more detail elsewhere [37].

4. Summary

It has been demonstrated that the capability of the modulated-temperature DSC (DDSC) to discriminate the simultaneous thermal responses of a reversible reaction from a non-reversible reaction enables the assessment of the glass transition temperature in Al-Y-Fe and Al-Sm melt-spun ribbons. In many Al-base amorphous alloys where glass formation appears the be controlled largely by the suppression of the growth of nuclei formed during rapid melt quenching, the calorimetric signal of glass transition is often obscured by the exothermic response from primary crystallization during continuous heating DSC. The observed glass transition temperature in the alloys under study by DDSC provides evidence that glassy state has actually been achieved in the systems through rapid solidification processing. Numerical value of the glass transition temperature is an important parameter in designing suitable annealing treatments that allow for the development of desired microstructures to yield optimized properties. In addition, numerical simulation reveals that heterogeneous transient nucleation on the high number quenched-in sites appears to be the nucleation mechanism in these metallic glasses during isothermal annealing. The growth of the high density Al nanocrystals during primary crystallization results solute rejection that in turn yields diffusion field impingement between neighboring that impedes growth significantly. The solute rejection also modifies the amorphous matrix composition and may provide for an enhanced thermal stability.

5. Reference

[1] A. Inoue, K. Ohtera, A. Tsai, and T. Masumoto, *Jap. J. Appl. Phy.*, **27** (1988) L479.

[2] A. Inoue, N. Matsumoto, and T. Masumoto, *Mater. Trans. JIM*, **31** (1990) 493.

[3] H. Chen, Y. He, G. J. Shiflet, and S. J. Poon, *Scripta Mater.*, **25** (1991) 331.

[4] Y. He, G. M. Dougherty, G. J. Shiflet, and S. J. Poon, *Acta Metall. Mater.*, **41** (1993) 337.

[5] A. L. Greer, *Science*, **267** (1995) 1947.

[6] G. P. Johari, S. Ram, G. Astl, and E. Mayer, *J. Non-Cryst. Solids*, **116** (1990) 2282.

[7] L. C. Chen and F. Spaepen, *Mater. Sci. Eng.*, **A133** (1991) 342.

[8] P. Schumacher and A. L. Greer, *Mater. Sci. Eng.*, **A178** (1994) 309.

[9] L. Battezzati, M. Baricco, P. Schumacher, W. C. Shih, and A. L. Greer, *Mater. Sci. Eng.*, **A179-180** (1994) 600.

[10] D. R. Allen, J. C. Foley, and J. H. Perepezko, *Acta Mater.*, **46(2)** (1998) 431.

[11] P. Rizzi, C. Antonione, M. Baricco, L. Battezzati, L. Armelao, E. Tondello, M. Fabrizo, and S. Daolio, *Nanostruct. Mater.*, **10** (1998) 767.

[12] Y. K. Kim, J. R. Soh, D. K. Kim, and H. M. Lee, *J. Non-Cryst. Solids*, **242** (1998) 122.

[13] Y. He, H. Chen, G. J. Shiflet, and S. J. Poon, *Phil. Mag. Lett*, **61** (1990) 297.

[14] Y. H. Kim, A. Inoue, and T. Masumoto, *Mater. Trans. JIM*, **31** (1990) 747.

[15] H. Chen, Y. He, G. J. Shiflet, and S. J. Poon, *Scripta Metall. Mater.*, **25** (1991) 1421.

[16] Y. H. Kim, A. Inoue, and T. Masumoto, *Mater. Trans. JIM*, **32** (1991) 599.

[17] T. Gloriant and A. L. Greer, *Nanostruct. Mater.*, **10** (1998) 389.

[18] A. Inoue, K. Ohtera, A. Tsai, and T. Masumoto, *Jap. J. Appl. Phy.*, **27** (1998) L479.

[19] B. Cantor, *Advances in Nanocrystallization*, **307** (1999) 143.

[20] A. Inoue and H. Kimura, *Nanostruct. Mater.*, **11** (1999) 221.

[21] A. Inoue and H. Kimura, *Synthesis and Processing of Nanocrystalline Powder*, ed. D. L. Bourell, TMS, Warrendale, PA, 1996, p. 91.

[22] A. Inoue and T. Masumoto, *Amorphous Alloys*, Amsterdam: Elsevier Science Publ., 1993, p. 133.

[23] M. Reading, D. Elliott, and V. L. Hill, *J. Thermal Analy.*, **40** (1993) 949.

[24] J. E. K. Schawe, *Thermochimica Acta*, **260** (1995) 1.

[25]   G. Wilde, R. I .Wu, and J. H. Perepzko, in preparation.

[26]   Q. Li, E. Johnson, A. Johansen, and L. Sarholt-Kristensen, *Mater. Sci. Eng.*, **A151** (1992) 107.

[27]   J. C. Foley, D. R. Allen, and J. H. Perepezko, *Scripta Mater.*, **35** (1996) 655.

[28]   A. A. Csontos and G. J. Shiflet, *Nanostruct. Mater.*, **9** (1997) 281.

[29]   A. Inoue and C. Fan, *Nanostruct. Mater.*, **12** (1999) 741.

[30]   J. C. Foley, D. R. Allen, and J. H. Perepezko, *Mater. Sci. Eng.*, **A226-A228** (1997) 569.

[31]   D. Kashchiev, *Surf. Sci.*, **14** (1969) 209.

[32]   K. F. Kelton, A. L. Greer, and C. V. Thompson, *J. Chem. Phys.*, **79** (1983) 6261.

[33]   M. Buchwitz, R. Adlwarth-Dieball, and P. L. Ryder, *Acta Metall. Mater.*, **41** (1993) 1885.

[34]   J. C. Foley, PhD-Thesis, UW-Madison, 1997.

[35]   G. Wilde, H. Sieber, and J. H. Perepezko, *J. Non-Cryst. Solids*, **250-252** (1999) 621.
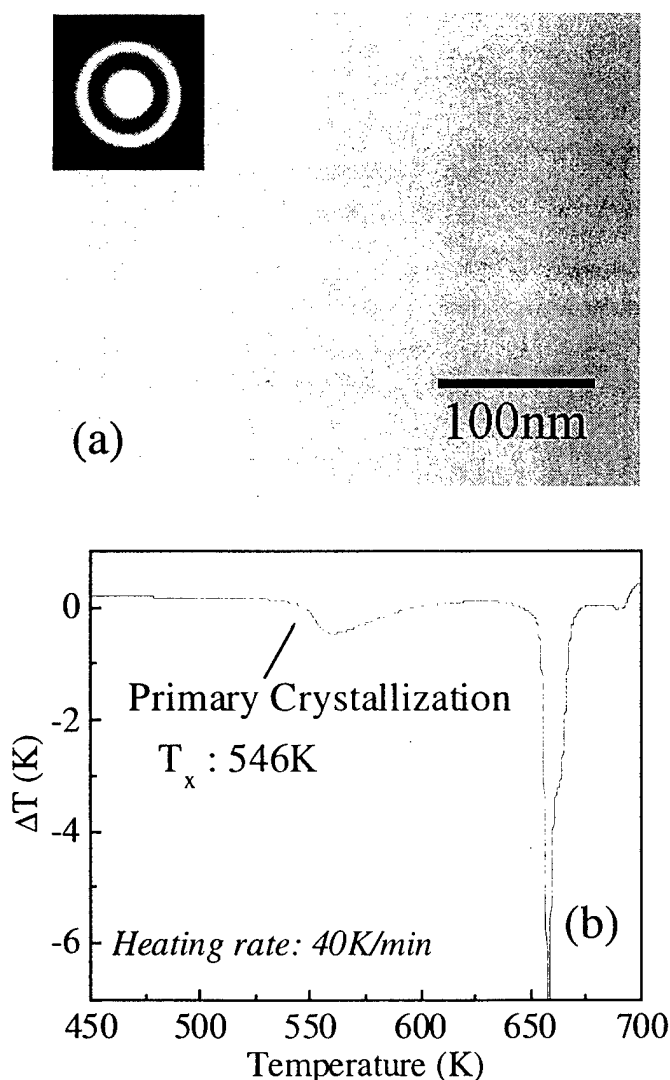
Figure 1: TEM bright-field image of as-spun $Al_{88}Y_7Fe_5$ (a). The inset shows the corresponding SAED pattern that indicates the absence of a detectable crystalline fraction. The DSC trace (b) exhibits a primary crystallization peak but no glass transition is observed.
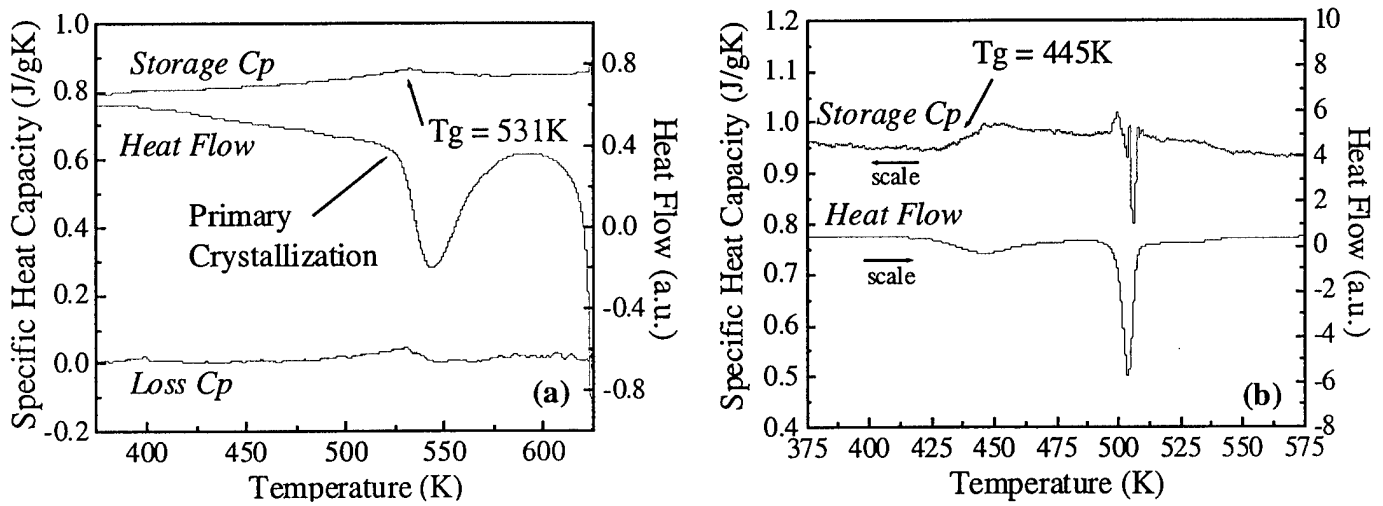
Figure 2: Results of the modulated-temperature DSC results on the as-spun sample of (a) $Al_{88}Y_7Fe_5$ and (b) $Al_{92}Sm_8$. The glass transition temperatures (T_g) were obtained as 531K in (a) [25] and 445K in (b), respectively.
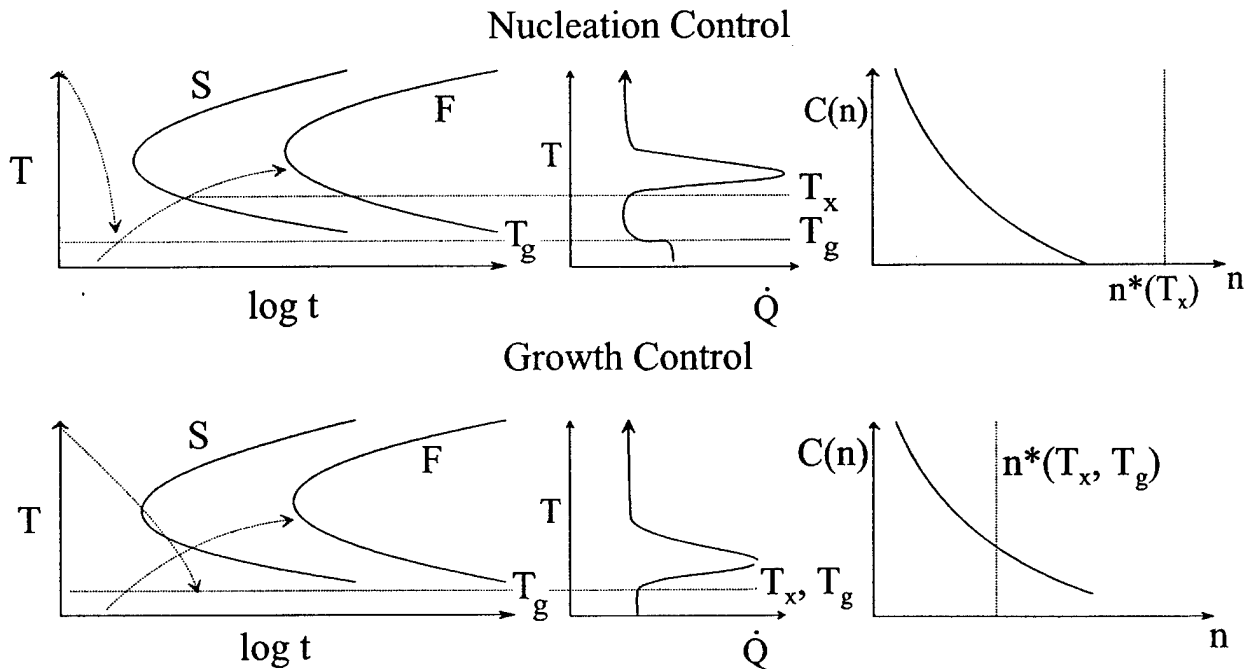

Figure 3: Schematics showing kinetics of metallic glass formation: nucleation control vs. growth control. Quenching and reheating paths are shown on the TTT diagrams (S-start; F-finish) and thermograms (dQ/dt: heat evolution rate).
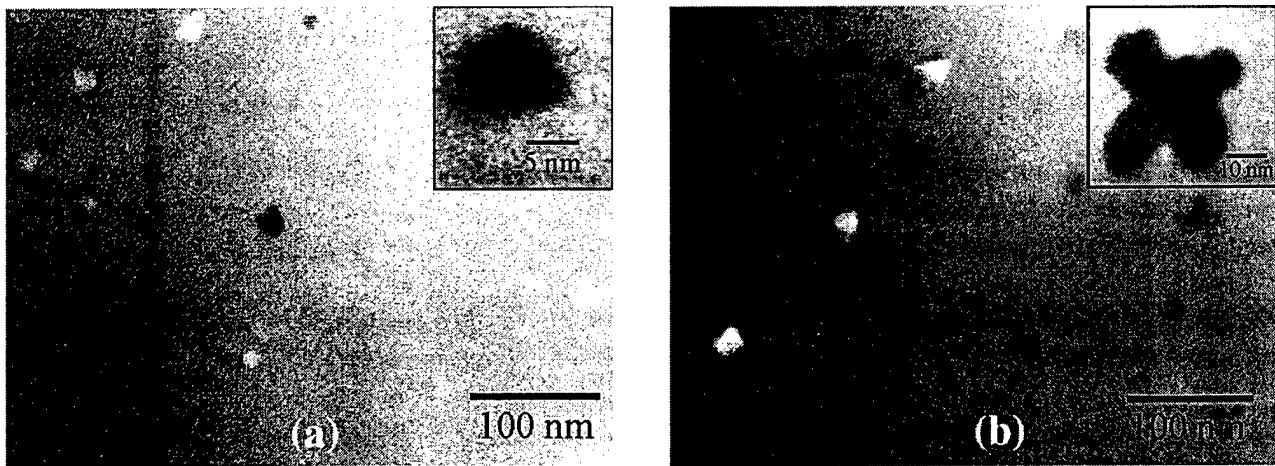
Figure 4: TEM bright-field images of an $Al_{88}Y_7Fe_5$ melt-spun sample after isothermal annealing at 518K for 10min (a) showing a high density $(3 \times 10^{21} m^{-3})$ of Al nanocrystals with nearly spherical shape; and 30min (b) showing higher particle density $(4.8 \times 10^{21} m^{-3})$ of Al nanocrystals and the development of a dendritic morphology.
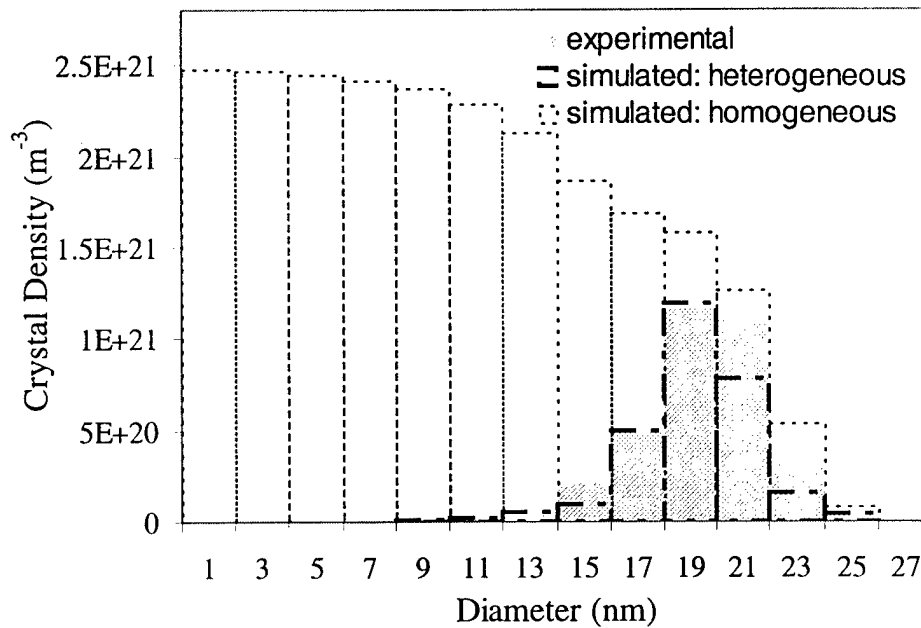

Figure 5: The size distribution of Al nanocrystals for the $Al_{88}Y_7Fe_5$ melt-spun sample isothermally annealed at 518K for 10 minutes plotted with the simulated distribution for homogeneous and heterogeneous nucleation.

6. List of Publications during the reporting period

1. "Strategies for the Development of Nanocrystalline Materials Through Devitrification", J.C. Foley, D.R. Allen and J.H. Perepezko, Mat. Sci and Eng. A, 226-228, 569 (1997).

2. "The Effect of Processing on Microstructural Evolution during Solidification of Al-7Y-5Fe Glass Forming Alloys", J.C. Foley, H. Sieber, D.R. Allen and J.H. Perepezko, Solidification Processing 1997, Eds. J. Beech and H. Jones (Dept. Engr. Mats., Univ. of Sheffield, UK) 602 (1997).

3. "Nanocrystal Development During Primary Crystallization of Amorphous Alloys", D. R. Allen, J.C. Foley and J. H. Perepezko, Acta Mater. 46, 431 (1998).

4. "Initial Crystallization Reactions", J.H. Perepezko and D.R. Allen, Mat. Res. Soc. Symp. Proc.,580, 221 (2000).

5. "Solidification of Atomized Liquid Droplets", J.H. Perepezko, J.L. Sebright and P.G. Höckel, "Liquid Metal Atomization: Fundamentals and Practice", Eds. K.P. Cooper, I.E. Anderson, S.D. Ridder and F.S. Biancaniello (TMS, Warrendale, PA) p.243 (2000).

6. "Glass Formation and Primary Nanocrystallization in Al-Base Metallic Glasses", R.I. Wu, G. Wilde and J.H. Perepezko, Nanostructured Materials (in press).

7. "Synthesis and Stability of Amorphous Al Alloys", J.H. Perepezko, R.I. Wu, R. Hebert and G. Wilde, Mat.Res.Soc.Symp.Proc. (in press).

7. Participating Scientific Personnel

   a. Professor J.H. Perepezko, Principal Investigator

   b. J. C. Foley, Graduate Student, (Phd, Materials Science and Engineering, 12/97)

   c. D.R. Allen, Graduate Student, (Phd, Materials Science and Engineering, 12/98)

   d. J. L. Sebright, Graduate Student, (MS, Materials Science, 5/00)

(Note: All graduate students are U.S. citizens).

8. Report of Inventions : None during the period